Ionic-Strength-Dependent Effects in Protein Folding: Analysis of Rate Equilibrium Free-Energy Relationships and Their Interpretation†

Benben Song,‡ Jae-Hyun Cho,§ and Daniel P. Raleigh*,‡,§,||

Department of Chemistry, State University of New York at Stony Brook, Stony Brook, New York 11794-3400, Graduate Program in Biochemistry and Structure Biology, State University of New York at Stony Brook, Stony Brook, New York 11794, and Institute for Chemical Biology and Drug Discovery, State University of New York at Stony Brook, Stony Brook, New York 11794-3400

Received August 14, 2007; Revised Manuscript Received October 1, 2007

ABSTRACT: The traditional approach to studying protein folding involves applying a perturbation, usually denaturant or mutation, and determining the effect upon the free energy of folding, ΔG^0, and the activation free energy, $\Delta G^{\neq}$. Data collected as a function of the perturbation can be used to construct rate equilibrium free-energy relationships, which report on the development of interactions in the transition state for folding. We examine the use of the ionic-strength-dependent rate equilibrium free-energy relationship in protein folding using the N-terminal domain of L9, a small $\alpha-\beta$ protein, as a model system. Folding is two-state for the range of ionic strength examined, 0.045−1.52 M. The plot of $\Delta G^{\neq}$ versus ΔG^0 is linear (r^2= 0.918), with a slope equal to 0.45. The relatively low value of the slope indicates that the ionic-strength-dependent interactions are modestly developed in the transition state. The slope is, however, greater than that of a plot of $\Delta G^{\neq}$ versus ΔG^0 constructed by varying pH, thus demonstrating directly that ionic-strength-dependent studies probe more than simple electrostatic interactions. Potential transition movement was probed by analysis of the denaturant, ionic strength cross-interaction parameters. The values are small but nonzero and positive, suggesting a small shift of the transition state toward the native state as the protein is destabilized, i.e., Hammond behavior. The complications that arise in the interpretation of ionic-strength-dependent rate equilibrium free-energy relationships are discussed, and it is concluded that the ionic-strength-dependent studies do not provide a reliable indicator of the role of electrostatic interactions. Complications include incomplete screening of electrostatic interactions, specific ion binding, Hofmeister effects, and the potential presence of electrostatic interactions in the denatured state ensemble.

The characterization of the structure and energetics of the transition-state ensemble (TSE)[1] is a central issue in biophysical studies of protein folding, particularly for single-domain structures, which fold in a two-state fashion (*1*−*5*). Experimental investigations often make use of so-called rate equilibrium free-energy relationships (REFERs) (*6*−*9*). In the simplest case, a linear relationship is observed between the change in the logarithm of the folding rate, ln k_f, with a perturbation and the change in the logarithm of the equilibrium constant, ln K, with the same perturbation. The ratio

$$\alpha_x = \frac{\partial \ln k_f/\partial x}{\partial \ln K/\partial x} \quad (1)$$

defines the interaction parameter α, where x denotes the perturbation. The observation of constant α_x values over a broad range of ΔG^0 argues that the barrier is narrow and well-defined along the reaction coordinate being probed (*6*, *9*). Nonlinear relationships between $\Delta G^{\neq}$ and ΔG^0 can also be observed. Nonlinearities can result from a variety of factors: (i) the movement of the transition state along a broad barrier, (ii) a change in the rate-limiting step of a sequential pathway, (iii) changes in parallel pathways, and (iv) a change of one or both of the ground states induced by the perturbation (*6*).

If x is the concentration of the denaturant, the relationship is simply the well-known Tanford β parameter (β_T or θ_m), which defines the position of the TSE relative to a dimensionless order parameter that reports upon the relative compactness of the transition state (*10*). Other examples albeit less commonly employed ones, include temperature, pressure, and pH. Temperature-dependent studies define α_T, which is equal to $\Delta S^{\neq}/\Delta S^0$, where $\Delta S^{\neq}$ is the activation entropy and ΔS^0 is the equilibrium change in entropy (*11*−*13*). Pressure-dependent studies yield $\alpha_p = \Delta V^{\neq}/\Delta V^0$ and probe the change in volume of the system at the TSE, $\Delta V^{\neq}$, relative to the total volume change associated with folding, ΔV^0 (*14*). pH-dependent investigations provide a global view of the development of interactions involving titratable groups (*15*−*17*). α_{pH} is formerly equal to $\Delta Q^{\neq}/\Delta Q^0$, where $\Delta Q^{\neq}$ is the difference in the number of protons bound to the TSE and denatured state ensemble (DSE), while ΔQ^0 is the difference between the number of protons bound to the folded

† This work was supported by NIH Grant GM 70941.

* To whom correspondence should be addressed. Telephone: (631) 632-9547. Fax: (631) 632-7960. E-mail: draleigh@notes.cc.sunysb.edu.

‡ Department of Chemistry.

§ Graduate Program in Biochemistry and Structure Biology.

|| Institute for Chemical Biology and Drug Discovery.

[1] Abbreviations: DSE, denatured state ensemble; K, equilibrium constant for protein folding; I, ionic strength; k_f, rate constant for protein folding; m_{eq}, slope of a plot of ln K versus the denaturant concentration; m_f, slope of a plot of ln(k_f) versus the denaturant concentration; NTL9, N-terminal domain of ribosomal protein L9 from *Bacillus stearothermophilus*, corresponding to residues 1−56; REFER, rate equilibrium free-energy relationship; TSE, transition-state ensemble; α_x, value of $(\partial\Delta G^{\neq}/\partial x)/(\partial\Delta G^0/\partial x)$, where x represents a perturbation; β_T, Tanford β value ($=m_f/m_{eq}$); θ_m, alternative notation used for the Tanford β value.

10.1021/bi701645g CCC: $37.00
Published on Web 11/15/2007

state and the protons bound to the DSE. The concept can be extended to include mutations as a perturbation (*2*, *3*, *6*, *17*). Within this context, the commonly employed φ values, $\varphi = \Delta\Delta G^{\neq}/\Delta\Delta G^{0}$, can be viewed as a linear REFER defined by two points, the wild type and mutant.

φ values are widely used in protein folding to probe the development of interactions at the level of individual residues and can, if denatured state effects are not important, be used to define the fractional development of side-chain interactions (*1*−*3*, *6*, *17*, *18*). The φ-value methodology has been applied to a large number of proteins, and β_T has been measured for even more. There have been surprisingly few investigations of the development of electrostatic interactions during protein folding despite the fact that they can be important for stability and can play a key role in specifying a unique structure (*15*, *16*, *19*−*32*). A number of investigations have relied on the pH dependence of protein folding to probe the development of electrostatic interactions (*15*, *16*, *19*, *20*, *23*). Complimentary information might, in principle, be obtained from ionic-strength-dependent studies; however, these have been relatively rare (*33*−*37*). Furthermore, their analysis can be complicated because variation in the ionic strength can affect more than charge−charge interactions; specific binding may occur, and Hofmeister effects might contribute (*26*, *36*−*41*). There is another important but often unappreciated additional complication with the analysis of ionic-strength-dependent studies, namely, that not all charge−charge interactions will be equally screened by salt even if the interacting groups lie on the surface of the protein. Interactions involving well-separated charges are screened more effectively than those involving charges that are in close proximity, and there are even examples of charge−charge interactions that are not screened by salt. This effect has been observed independently by several groups in both computational and experimental studies (*41*−*43*). In a qualitative sense, this can arise if the groups in question lie close to each other and the ion cloud does not interpenetrate.

Application of the REFER approach to ionic-strength-dependent studies offers the advantage that it does not depend upon the assumption of a particular physical model, such as, for example, a Debye−Hükel-type approach, or the validity of a particular theory of ionic solutions (*33*). The REFER analysis has not yet been applied to ionic-strength-dependent studies of protein folding. In the present work, we analyze the ionic strength dependence of the folding of a small $\alpha-\beta$ protein, the N-terminal domain of the ribosomal protein L9 (NTL9), and show that ionic strength can be used to define a REFER. NTL9 has been the subject of extensive folding studies, and the development of electrostatic interactions in the TSE have been characterized by pH-dependent studies (*13*, *19*, *32*, *43*−*45*). Thus, NTL9 offers an ideal test case to assess if ionic-strength-dependent REFERs can be interpreted in terms of the development of just electrostatic interactions. The folding of NTL9 has been well-studied by more traditional approaches, and the folding of the core split $\beta-\alpha-\beta$ motif is two-state over a wide range of conditions, making it a useful model system for biophysical studies.

MATERIALS AND METHODS

Protein Expression and Purification. NTL9 was overexpressed in the BL21(DE3) strain of *Escherichia coli* and purified by ion-exchange chromatography and reverse-phase high-performance liquid chromatography (HPLC) as previously described, with the exception that trifluoroacetic acid (TFA) was avoided during the HPLC purification stage (*30*). TFA is difficult to remove, and we wanted to avoid variations in ionic strength because of the associated TFA counterion. The identity of the peptide was confirmed by matrix-assisted laser desorption ionization time-of-flight (MALDI−TOF) mass spectrometry (expected, 6219.3; observed, 6218.9).

Protein-Stability Measurements. Protein stability was determined by chemical denaturation monitored by circular dichroism (CD) at 222 nm. Measurements were made using an Aviv Instrument model 202SF spectrometer. Denaturation experiments were performed in 20 mM sodium acetate (NaAc) buffer with different salt concentrations at pH 5.5 and 25 °C. The protein concentration was about 20 μM. Urea was chosen as the denaturant because it is non-ionic. The data from chemical denaturation experiments were fit as plots of ellipticity versus the denaturant concentration to the following equation:

$$\theta = (a_n + b_n[\text{denaturant}]) + \frac{(a_d + b_d[\text{denaturant}]e^{-(\Delta G^0[\text{denaturant}])/RT})}{1 + e^{-(\Delta G^0[\text{denaturant}])/RT}} \quad (2)$$

where θ is the ellipticity, T is the temperature, R is the gas constant, ΔG^0 is the free energy of unfolding, a_n and b_n are used to define the ellipticity of the native state, and a_d and b_d are used to define the ellipticity of the denatured state. The free energy of unfolding is assumed to be a linear function of the denaturant concentration (*46*, *47*)

$$\Delta G^0 = \Delta G^0(H_2O) - m_{eq}[\text{denaturant}] \quad (3)$$

The linear relationship has been shown to be valid for NTL9 (*44*). At the highest salt concentrations, the curves did not have good post-transition baselines, making the fits difficult. In these cases, the stability was estimated by determining the concentration of urea at the midpoint, c_M, by numerically differentiating the curve. $\Delta G^0(H_2O)$ was calculated via

$$\Delta G^0(H_2O) = c_M m_{avg} \quad (4)$$

where m_{avg} is the average m value for data collected between 0 and 1.0 M added salt. The ionic strength of the solutions was calculated using the standard expression

$$I = \frac{1}{2}\sum_k m_k z_k^2 \quad (5)$$

where m_k is the molar concentration and z_k is the valency of ionic species k.

Kinetic Folding Studies. Protein folding and unfolding rates were determined by fluorescence stopped-flow experiments using an Applied Photophysics Model SX.18MV instrument. The fluorescence signal of the single tyrosine at position 25 of NTL9 was followed. The excitation wavelength was 280 nm, and the fluorescence signal above 305 nm was recorded using a cutoff filter. All experiments were done in a 20 mM sodium acetate buffer at pH 5.5 with different salt concentrations at 25 °C. Final protein concentrations were about 50 μM. For refolding studies, the peptide

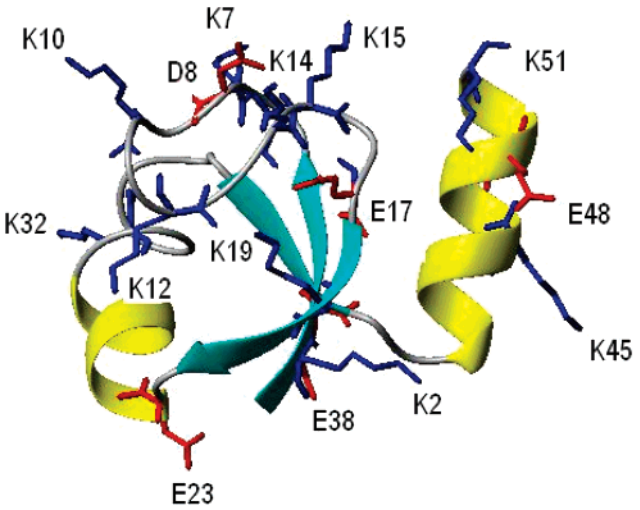

FIGURE 1: Ribbon diagram of NTL9. The acidic and basic residues are shown in a stick format. The diagram was constructed using the PDB file 2HBB and MolMol. The last few residues of NTL9 are disordered in the X-ray structure. Thus, the position of Glu54 and the C terminus are not shown.

was dissolved in 9−10 M urea and folding was initiated by mixing with 10 volumes of buffer with a low concentration of denaturant. For unfolding studies, the peptide was dissolved in native buffer and unfolding was initiated by mixing with solutions of a high denaturant concentration. Four or five fluorescence traces were typically averaged at each concentration of denaturant. The resulting trace was fit to a single exponential to determine the observed rate constant (k_{obs}). Plots of ln k_{obs} versus the denaturant concentration, so-called chevron plots, were fit to the following equation to obtain the folding and unfolding rates in the absence of the denaturant:

$$\ln(k_{obs}) = \ln(k_f^{H_2O} e^{-(m_f[\text{denaturant}])} + k_u^{H_2O} e^{(m_u[\text{denaturant}])}) \quad (6)$$

where $k_u^{H_2O}$ and $k_f^{H_2O}$ are the unfolding and folding rates in the absence of the denaturant, m_f and m_u describe how ln(k_f) and ln(k_u) are dependent upon the concentration of the denaturant. m_f is widely thought to report on the change in solvent-accessible surface area between the DSE and TSE, while m_u reports on the change in surface area between the native state and TSE (*10*, *47*). Only the folding branch was collected at higher concentrations of salt because the unfolding branch is so small that the fitted parameters k_u and m_u are not reliable.

RESULTS AND DISCUSSION

NTL9 as a Model System. NTL9 is a basic protein with 11 Lys, 1 Arg, and 6 acidic residues. The domain forms one of the simplest examples of the split $\beta-\alpha-\beta$ motif (Figure 1). The fold consists of a three-stranded antiparallel β sheet with a short α helix connecting strands two and three. The ordered loop connecting the first and second β strand is rich in Lys. The second helix forms the long interdomain connector between the N- and C-terminal domains. The construct used here consists of residues 1−56 of the intact protein. The final few residues of the C-terminal helix are frayed in solution (*45*). The acidic residues in NTL9 are well-distributed across the surface, and only one, D23, appears to be involved in a well-defined pairwise interaction, namely, a salt bridge with the N terminus (Figure 2) (*43*). Analysis of the native state pK_a values shows that D8, E17, and D23 have pK_a values below model compound values, indicating that they are involved in favorable electrostatic interactions in the native state (*27*). A surface representation coded by charge is displayed in Figure 2.

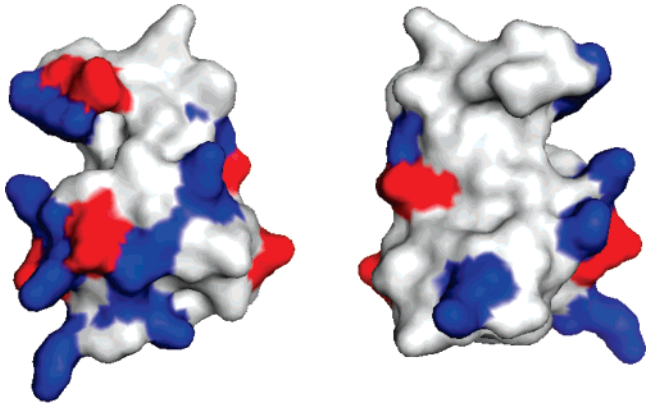

FIGURE 2: Color-coded surface representation of NTL9 showing the distribution of positively charged (blue) and negatively charged (red) residues. A and B differ by 180° rotation around the *z* axis.

Stability Studies. The stability of NTL9 was measured by CD-monitored urea denaturation as a function of the salt concentration over a range of 0−1.5 M. A total of 21 different measurements were made at 10 different values of the ionic strength. Urea was used because guanidine HCl is a salt and will change the ionic strength. All experiments were performed at pH 5.5 because previous folding studies were conducted at this pH. NTL9 is a small protein and this leads to a relatively broad urea-induced unfolding transition, that, in turn, causes problems with the post-transition baselines at the highest salt concentration. The stability was determined by directly fitting the curve to eq 2 for salt concentrations below 1.0 M. The midpoint of the urea-induced unfolding transition, c_m, can be estimated even with a poor post-transition baseline. This allows for the stability at high salt concentration to be determined using eq 4 and the average value of m_{eq}. The equilibrium m value, m_{eq}, is independent of the ionic strength to within the experimental precision. The m_{eq} value is related to the change in solvent-accessible surface area between the native state and DSE. The observation that the m_{eq} value is independent of the ionic strength argues that there is no significant change in the compactness of the DSE at a high salt concentration. At first glance, this may seem surprising because the DSE of NTL9 is expected to have a net charge near +6 at pH 5.5, and thus, reduction of electrostatic interactions via screening might be expected to lead to compaction. However, there are also specific electrostatic interactions that favor a compact DSE, and these too should be screened by a high salt concentration favoring expansion at high salt (*27*, *32*). Thus, the two competing effects conspire to reduce the dependence of m_{eq} on the ionic strength. The stability increased from 4.16 to 5.53 kcal/mol over the range of salt concentrations studied, indicating that ionic-strength-dependent interactions make a net unfavorable contribution to ΔG^0 under these conditions (Table 1). Plots of the apparent fraction of unfolded versus [urea] at different salt concentrations are shown in Figure 3. The plots of ellipticity versus [urea] together with the associated fits are included in the Supporting Information.

Table 1: Summary of the Kinetic and Thermodynamic Data[a]

added salt[b]	ΔG^{0} [c] (kcal mol^{-1})	m_{eq} (kcal mol^{-1} M^{-1})	k_f (s^{-1})	m_f (kcal mol^{-1} M^{-1})	β_T
no salt	4.16 ± 0.040	0.65 ± 0.010	820 ± 30.0	0.44 ± 0.010	0.67 ± 0.010
			760 ± 20.0	0.45 ± 0.010	0.69 ± 0.010
			750 ± 30.0	0.41 ± 0.010	0.63 ± 0.010
0.025 M NaCl	4.21 ± 0.120	0.65 ± 0.020	820 ± 40.0	0.44 ± 0.010	0.67 ± 0.010
0.05 M NaCl	4.15 ± 0.070	0.63 ± 0.010	910 ± 20.0	0.45 ± 0.010	0.71 ± 0.010
			860 ± 30.0	0.44 ± 0.010	0.69 ± 0.010
0.1 M NaCl	4.34 ± 0.080	0.66 ± 0.010	950 ± 30.0	0.46 ± 0.010	0.69 ± 0.010
			990 ± 40.0	0.47 ± 0.010	0.71 ± 0.010
0.15 M NaCl	4.20 ± 0.070	0.63 ± 0.010	840 ± 30.0	0.42 ± 0.020	0.66 ± 0.020
0.25 M NaCl	4.62 ± 0.040	0.67 ± 0.010	900 ± 30.0	0.40 ± 0.010	0.59 ± 0.010
0.5 M NaCl	4.70 ± 0.040	0.66 ± 0.010	1190 ± 70.0	0.43 ± 0.010	0.65 ± 0.010
0.75 M NaCl	5.04 ± 0.090	0.68 ± 0.010	1450 ± 140.0	0.42 ± 0.010	0.61 ± 0.010
1 M NaCl	5.05 ± 0.050	0.66 ± 0.010	1880 ± 170.0	0.43 ± 0.010	0.65 ± 0.010
1.5 M NaCl	5.53 ± 0.060	0.66 ± 0.010	2060 ± 110.0	0.40 ± 0.010	0.60 ± 0.010
			2580 ± 120.0	0.42 ± 0.010	0.63 ± 0.010
0.1 M NaAc	4.50 ± 0.320	0.66 ± 0.060	1060 ± 30.0	0.46 ± 0.010	0.69 ± 0.040
0.1 M NaF	4.47 ± 0.200	0.67 ± 0.030	1040 ± 30.0	0.46 ± 0.010	0.68 ± 0.010
0.1 M KCl	4.41 ± 0.200	0.68 ± 0.030	1030 ± 30.0	0.47 ± 0.010	0.69 ± 0.010
0.75 M KCl	4.99 ± 0.050	0.72 ± 0.080	1370 ± 140.0	0.48 ± 0.020	0.66 ± 0.040
0.033 M Na_2SO_4	4.45 ± 0.120	0.65 ± 0.030	860 ± 40.0	0.46 ± 0.010	0.70 ± 0.020
0.25 M Na_2SO_4	4.75 ± 0.04	0.71 ± 0.060	1240 ± 90.0	0.43 ± 0.010	0.60 ± 0.040

[a] Studies were conducted in 20 mM NaAc at pH 5.5 and 25 °C. [b] All samples contained 20 mM NaAc in addition to the added salt. Thus, the ionic strength is 20 mM larger than the values determined by the listed salt concentration. The numbers after the ± symbol represent the standard error to the fit. [c] Determined from equilibrium unfolding as described in the Materials and Methods.

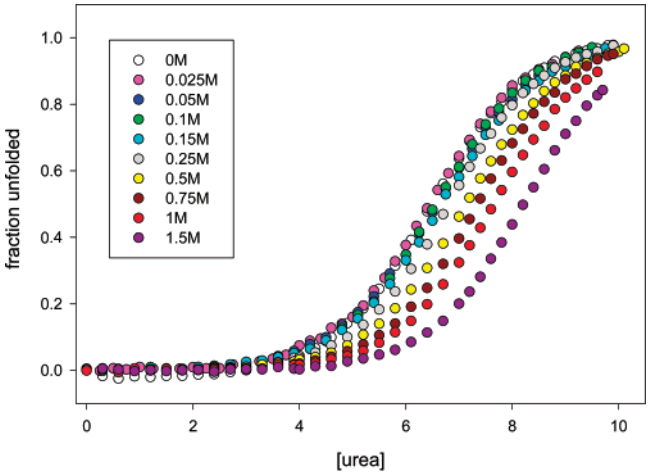

FIGURE 3: Plots of the fraction of unfolded versus [urea] at various concentrations of NaCl. The ionic strength increases from left to right. Measurements were made in 20 mM sodium acetate at pH 5.5 and 25 °C. The concentration of added NaCl were 0, 0.025, 0.05, 0.1, 0.15, 0.25, 0.5, 0.75, 1, and 1.5 M from left to right.

Salts can modulate protein stability by changes in the ionic strength, by specific binding, and via Hofmeister effects (*26*, *28*, *36*−*40*). In theory, although often not in practice, the functional form of the dependence of ΔG^0 upon the ionic strength, I, yields information about the mechanism of ionic strength effects. Specific binding leads to a linear dependence of ΔG^0 upon I when the ligand concentration is above k_d. Evidence against specific binding is provided by studies that examined the effect of varying the anion and cation. It is easy to vary the cation using KCl. Variation of the anion is more problematic because the absorbance of Br^- or I^- causes problems, and sulfate introduces complications because it nonspecifically stabilizes proteins via preferential exclusion. We conducted additional measurements at a total ionic strength of 120 mM using 20 mM sodium acetate with 100 mM KCl, 100 mM NaBr, 100 mM NaF, 100 mM NaAc, and 33 mM Na_2SO_4. The measured stability was in excellent agreement with that determined using NaCl to adjust the ionic strength (Table 1). Additional measurements were made at 770 mM total ionic strength using 750 mM KCl and 250 mM Na_2SO_4. The agreement with the NaCl data is good.

The ionic strength dependence of electrostatic screening is complicated. Some workers have used a simple Debye−Hükel limiting law $\sqrt{I}$ dependence expected for the activity coefficient of an ion at very dilute salt concentrations (*33*). It is not at all obvious why such a relationship should be expected to describe the variation of ΔG^0 with the ionic strength over the range of salt concentrations used in protein stability studies. It is also worth bearing in mind that it can be difficult to distinguish between an $\sqrt{I}$ dependence and a linear dependence upon I, such as that expected for classic Hofmeister effects (*39*). Electrostatic screening has also been modeled using a Columbic potential with a Debye screening term derived from model-dependent solution of the linearized Poisson−Boltzmann equation (*42*)

$$U_c(r_{ij})e^{-\kappa r_{ij}} \quad (7)$$

where U_c is the columbic potential for two charges separated by a distance r_{ij} in a medium of dielectric constant ϵ. κ is the Debye parameter, which is related to the Debye screening length. κ is proportional to $\sqrt{I/\epsilon T}$, where I is the ionic strength and T is the absolute temperature. The relationship predicts that the screening of pairwise charge−charge interactions should have a $Ae^{-\sqrt{I}}$ dependence on the ionic strength, ignoring the small contribution from the salt effect on ϵ. This simple relationship has been successfully used to rationalize salt-dependent pK_a shifts even for salt concentrations well above the expected range of validity of the Debye−Hükel model. Note that eq 7 does not predict that ΔG^0 will decrease with an increasing ionic strength because both favorable and unfavorable electrostatic interactions will be screened. If the electrostatic free energy can be written

as the sum of a set of pairwise terms, then the effect of increasing the ionic strength should follow a $Ae^{-}\sqrt{I}$ dependence, where A is independent of the ionic strength. Figure 5 compares plots of ΔG^0 versus I, $\sqrt{I}$, and $Ae^{-}\sqrt{I}$. In all three cases, the data appear to be well-fit. The plot of ΔG^0 versus $\sqrt{I}$ appears linear, with a r^2 value of 0.904. Plotting ΔG^0 versus I also yields a linear plot, with $r^2 = 0.908$. Plotting ΔG^0 versus $Ae^{-}\sqrt{I}$ also yields a linear plot, with $r^2 = 0.873$. A comparison of the plots highlights the practical difficulty in distinguishing between an I or other dependence of ΔG^0 on the ionic strength. This is a general difficulty with ionic-strength-dependent studies and is not specific for NTL9. This is formally irrelevant to the REFER analysis.

Dependence of the Folding Rate upon Ionic Strength. The folding rate of NTL9 was determined for each of the samples used for the stability studies (Table 1). The rate increased with the ionic strength, although the effect upon ln k_f was less than the effect upon $\Delta G^0 - /RT$ (i.e., ln K). The effects of varying the composition of the salt were tested in exactly the same way as used for the stability studies. The effect on the rate constant varied with the ionic strength and not with the choice of salt for the points tested. Plots of the dependence of the natural logarithm of the observed first-order rate constant, ln k_{obs}, versus [urea], "chevron plots", collected at 0.1 and 1 M [NaCl] are shown in Figure 4. The plots have the typical V shape expected for two-state folding, with no observable rollover at a low denaturant concentration. The stability calculated from k_f and k_u is in good agreement with the values determined by equilibrium measurements: 4.12 kcal/mol from the kinetic measurements, 4.34 kcal/mol for the equilibrium measurements at 100 mM added salt, and 5.02 kcal/mol versus 5.05 kcal/mol for the kinetic and equilibrium values at 1 M NaCl. The m_{eq} values measured in the equilibrium studies are also in very good agreement with the values calculated from the kinetic parameters m_f and m_u.

A plot of ln k_f versus $\sqrt{I}$ is shown in Figure 6. The plot is well-fit to a straight line, with $r^2 = 0.900$. The data can also be fit to an $Ae^{-}\sqrt{I}$ dependence, with $r^2 = 0.845$. A linear dependence on I also nicely fits the data, with $r^2 = 0.918$, making it difficult to distinguish between classic Debye−Hükel behavior and an alternate salt dependence. Again, this highlights the difficulties in analyzing ionic-strength-dependent data, but once again, this is formally irrelevant for REFER analysis.

REFER Analysis of the Effects of the Ionic Strength. The data presented in the proceeding two subsections highlight the difficulties that can arise in trying to deduce if salt-dependent folding and/or stability data follow the Debye−Hükel relationship. The REFER analysis is not affected by these considerations because it simply seeks to deduce how ln k_f varies with ln K. A Leffler plot of ln k_f versus ln K is shown in Figure 7 (*6*, *48*, *49*). The parameter

$$\alpha_I = \left(\frac{\partial \Delta G^{\neq}}{\partial I}\right) / \left(\frac{\partial \Delta G^0}{\partial I}\right) \tag{8}$$

defines the ionic strength α value. There is an excellent linear relationship with slope, $\alpha_I = 0.45 \pm 0.030$, $r^2 = 0.918$. The modest value of α_I indicates that salt-dependent interactions

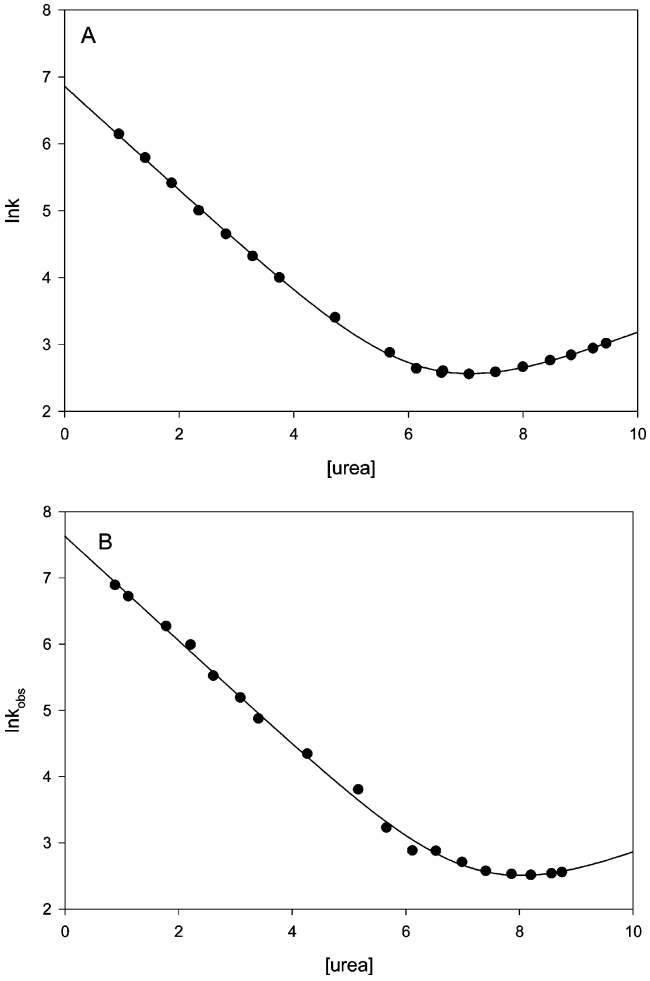

FIGURE 4: Plots of ln k_{obs} versus [urea], "chevron plots", for NTL9. (A) 100 mM NaCl and (B) 1 M NaCl. All experiments were conducted at pH 5.5 and 25 °C in 20 mM sodium acetate. Thus, the ionic strength was 0.12 M for A and 1.02 M for B.

are only partially developed in the transition state for folding. Interestingly, α_I is noticeable smaller than β_T (0.65) and $\Delta C_p^{\neq}/\Delta C_p$ (0.60), parameters which report on the burial of the surface area (*13*). However, the slope of the Leffler plot, α_I, is larger than $\alpha_{pH} = 0.33$, determined from pH-dependent studies (*19*).

There is, within the precision of the data, no hint of deviation from linearity in a plot of α_I versus ΔG_I^0. A linear plot is expected for narrow transition-state barriers; however, it can be difficult to detect deviations from linearity (*6*). Cross-interaction parameters can be more sensitive probes of transition-state movement (*6*, *9*). The cross-interaction parameter, α_{xy}, is defined by

$$\frac{\partial \alpha_x}{\partial \Delta G_y^0} = \frac{\partial^2 \Delta G^{\neq}}{\partial \Delta G_x^0 \partial \Delta G_y^0} \tag{9}$$

where the subscripts x and y refer to different perturbations (*6*). The data presented here can be used to calculate the cross-interaction parameter relating ionic strength and denaturant. Plots of α_I versus ΔG_{urea}^0 and β_T versus ΔG_I^0 are shown in Figure 8. The subscript urea indicates that the free energy is varied by changing the concentration of denaturant, and the subscript I indicates that ionic strength is used to change ΔG^0. The slope of the α_I versus ΔG_{urea}^0 plot is the

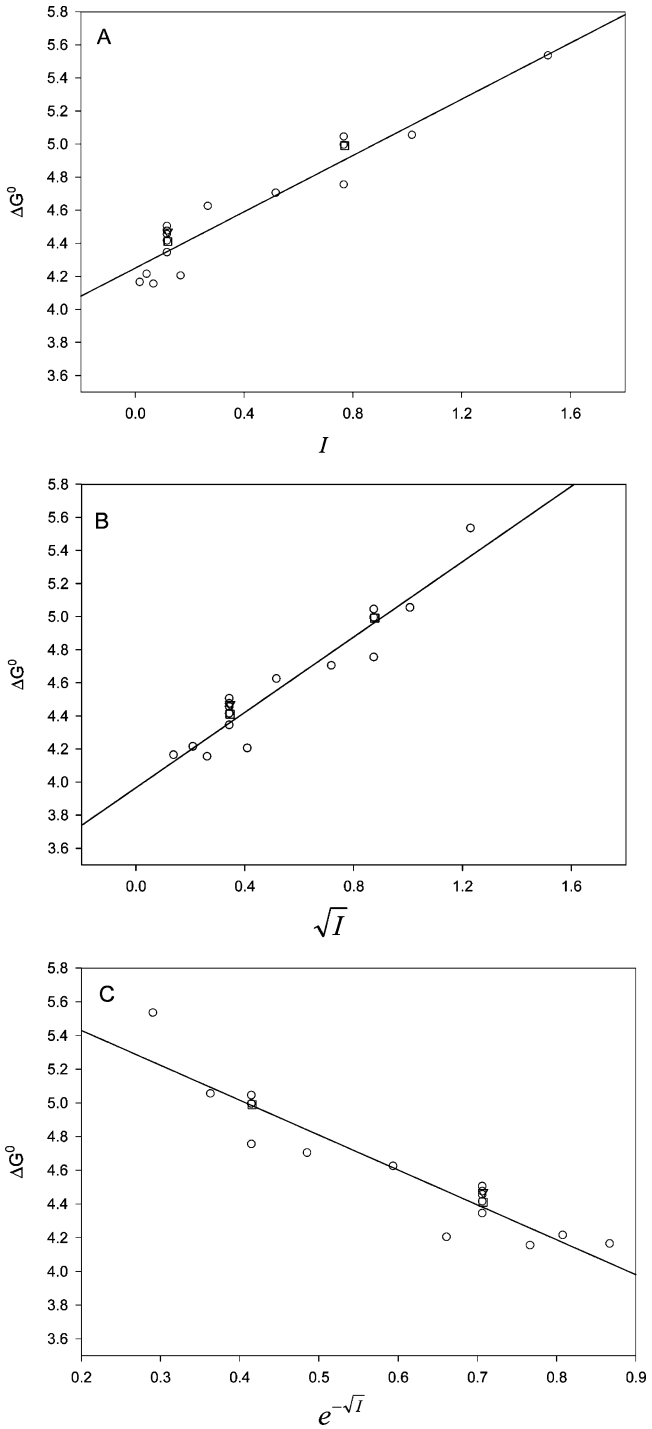

FIGURE 5: Plots of ΔG^0 versus (A) I, (B) $\sqrt{I}$, (C) $Ae^{-\sqrt{I}}$. Data were collected at pH 5.5 in 20 mM sodium acetate at 25 °C. NaCl-dependent data is indicated as ○; KCl-dependent data is indicated as □; and NaF-dependent data is indicated as ▽.

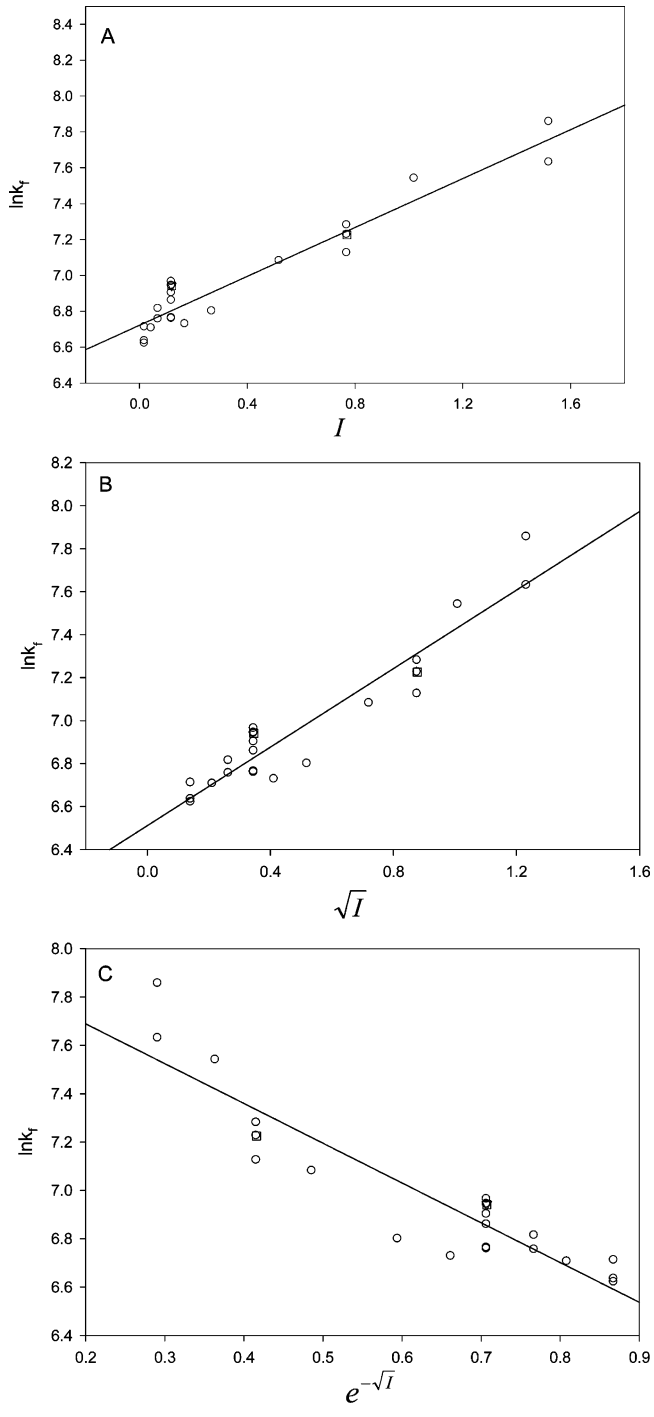

FIGURE 6: Plots of ln k_f versus (A) I, (B) $\sqrt{I}$, (C) $Ae^{-\sqrt{I}}$. Data were collected at pH 5.5 in 20 mM sodium acetate at 25 °C. NaCl-dependent data is indicated as ○; KCl-dependent data is indicated as □; and NaF-dependent data is indicated as ▽.

cross-interaction parameter $\partial^2\Delta G^{\neq}/\partial\Delta G^0_{urea}\partial\Delta G^0_I$, while the slope of the plot of β_T versus ΔG^0_I is $\partial^2\Delta G^{\neq}/\partial\Delta G^0_I\partial\Delta G^0_{urea}$. Both plots are linear with positive slope, although the scattering in the β_T versus ΔG^0_I plot coupled with the, necessarily, limited range of the data leads to a weak correlation ($r^2 = 0.404$). There is a strong correlation between α_I and ΔG^0_{urea} ($r^2 = 0.9997$). The slopes of the two plots are essentially equal as expected for cross-interaction parameters, and the magnitude of the slope is comparable to cross-interaction parameters determined in other systems (*6*). The positive cross-interaction parameters are consistent with the Hammond effect, i.e., movement of the transition state toward the native state upon destabilization.

CONCLUSIONS

The REFER analysis described here indicates that salt-dependent interactions are moderately developed in the transition state compared to the burial of the hydrophobic

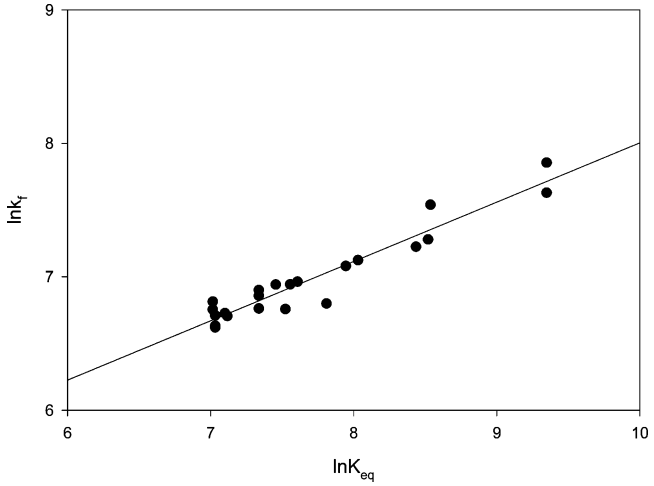

FIGURE 7: Leffler plot of ln k_f versus ln K for the ionic-strength-dependent data. The slope is 0.45, with r^2 =0.918.

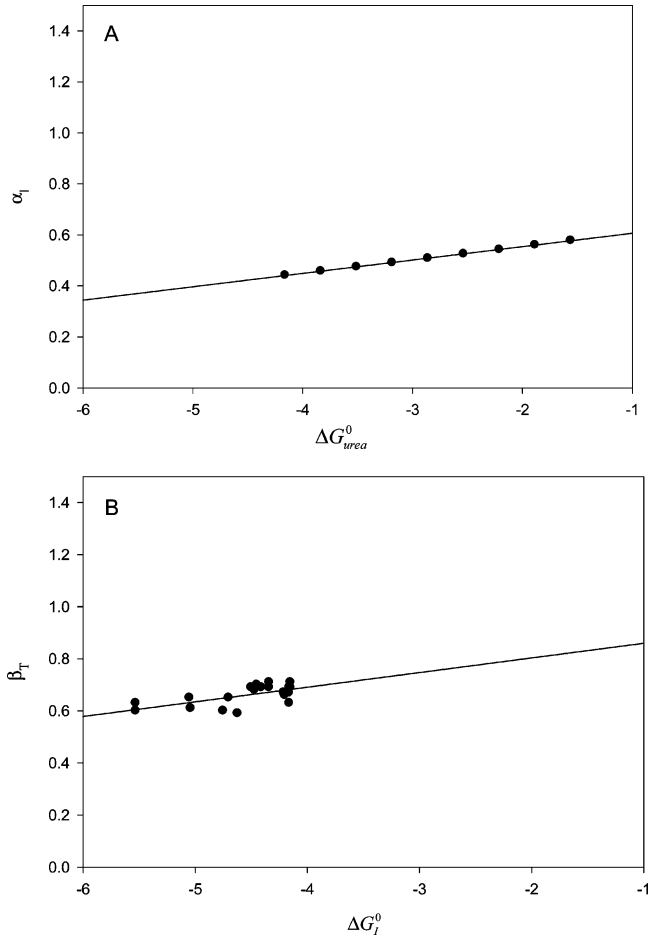

FIGURE 8: Analysis of cross-interaction parameters. (A) Plot of α_I versus ΔG^0_{urea}, slope = 0.052 mol kcal^{-1}, and r^2 = 0.9997. (B) Plot of β_T versus ΔG^0_I, slope = 0.056 mol kcal^{-1}, and r^2 = 0.404.

surface area. This seems reasonable because the charged residues in NTL9 all lie on the surface, while the hydrophobic groups are buried in the structure. Previous work involving modification of the hydrophobic core residues of NTL9 showed that there was an excellent correlation between the change in hydrophobicity caused by a modification and the change in the logarithm of the folding rate, while there was a much weaker relationship between the variation in the size and shape of the residues. This argues that the transition state involves the sequestering of hydrophobic groups while tight specific packing occurs on the downhill side of the barrier (*50*). Amide H/D isotope effect studies also indicate significant hydrogen-bonded structure in the transition state (*51*). When these studies are taken together, they suggest that the TSE of NTL9 contains a fairly well-structured backbone stabilized by a more loosely packed hydrophobic core. In this model, most of the charged residues are expected to be fluxional, solvated, and not involved in specific native interactions. In other words, in terms of solvation and conformational flexibility, the charged residues are in a more DSE-like environment rather than a native-like environment. There is at least one fairly specific interaction involving charged residues, which appears to be formed in the TSE. Mutational analysis of a set of Lys to Met and acidic to amide mutants showed that K12 and D8 are involved in non-native interactions in the DSE and indicated that these interactions are still present, although slightly weaker, in the TSE (*31*, *32*). The presence of non-native interactions in the TSE or DSE cannot be inferred directly from ionic-strength-dependent studies; however, this does not affect the REFER analysis. It can, however, affect the interpretation of the origins of any REFER. The persistence of this interaction contributes to the "DSE-like" character of the salt-sensitive interactions in the transition state.

A key question of interest is whether or not the salt dependence of the stability and activation free energy of NTL9 is due to screening of electrostatic interactions. It is clearly not easy to distinguish between a dependence on I versus a dependence of $\sqrt{I}$ or $Ae^{-}\sqrt{I}$, but nevertheless, we believe that part of the salt effects arise from screening, especially at low salt. First, the control experiments are consistent with a dependence on the total ionic strength and not the composition of the ion. This argues against specific ion binding as the origin of the observed effects. Second, the primary ions used, Na^+, K^+, Cl^-, and Br^-, all fall in the middle of the Hofmeister series and are relatively nonchaotropic and nonkosmotropic. These Hofmeister effects are expected to be modest at least for the lowest salt concentrations. They are expected to play a more important role as the salt concentration increases. On the other hand, pH-dependent studies yield an α_{pH} value of 0.33, which is clearly smaller than α_I. pH-dependent studies report on the development of electrostatic interactions and do not suffer from the same problems in interpretation that ionic-strength-dependent studies do. The larger value of α_I related to α_{pH} could arise from a contribution of nonelectrostatic interactions to the REFER, i.e., Hofmeister effects. These would be expected to increase α_I because, as described above, hydrophobic interactions play a key role in the folding of NTL9. Alternatively, α_I could be dominated by electrostatic screening but could still be different from α_{pH} because some interactions in the TSE or native state may not be screened by salt. Along these lines, it is interesting to note that the one specific pairwise charge−charge interaction in the native state, the salt bridge between the N terminus and D23, has been shown to be insensitive to screening by salt (*43*). Clearly, the common practice of assuming that ionic strength effects are only due to the screening of electrostatic interactions and that salt screens all electrostatic interactions equally is not correct.

The analysis of the cross-interaction parameters is consistent with a salt-induced Hammond effect. Finally, we note that the study described here illustrates the power of the REFER approach even when it is impossible to determine prior if ln k_f or ln K follows a Debye−Hükel-like relationship. In addition, the REFER analysis allows potential transition-state movement to be probed, and the variation of ionic strength provides a convenient method for measuring self- and cross-interaction parameters.

ACKNOWLEDGMENT

We thank Dr. Satoshi Sato and Ms. Rengin Soydaner for their contributions to the initial stages of this project and Ms. Humeyra Taskent for helpful discussions.

SUPPORTING INFORMATION AVAILABLE

Plots of ellipticity versus [urea] as a function of added salt, showing the individual fits. This material is available free of charge via the Internet at http://pubs.acs.org.

REFERENCES

1. Matthews, C. R. (1987) Effect of point mutations on the folding of globular proteins, *Methods Enzymol. 154*, 498−511.
2. Goldenberg, D. P., Frieden, R. W., Haack, J. A., and Morrison, T. B. (1989) Mutational analysis of a protein-folding pathway, *Nature 338*, 127−132.
3. Fersht, A. R., Matouschek, A., and Serrano, L. (1992) The folding of an enzyme. I. Theory of protein engineering analysis of stability and pathway of protein folding, *J. Mol. Biol. 224*, 771−782.
4. Itzhaki, L. S., Otzen, D. E., and Fersht, A. R. (1995) The structure of the transition state for folding of chymotrypsin inhibitor 2 analysed by protein engineering methods: Evidence for a nucleation−condensation mechanism for protein folding, *J. Mol. Biol. 254*, 260−288.
5. Jackson, S. E. (1998) How do small single-domain proteins fold, *Fold Des. 3*, R81−R91.
6. Sanchez, I. E., and Kiefhaber, T. (2003) Hammond behavior versus ground state effects in protein folding: Evidence for narrow free energy barriers and residual structure in unfolded states, *J. Mol. Biol. 327*, 867−884.
7. Matouschek, A., and Fersht, A. R. (1993) Application of physical organic chemistry to engineered mutants of proteins: Hammond postulate behavior in the transition state of protein folding, *Proc. Natl. Acad. Sci. U.S.A. 90*, 7814−7818.
8. Schatzle, M., and Kiefhaber, T. (2006) Shape of the free energy barriers for protein folding probed by multiple perturbation analysis, *J. Mol. Biol. 357*, 655−664.
9. Sanchez, I. E., and Kiefhaber, T. (2003) Non-linear rate-equilibrium free energy relationships and Hammond behavior in protein folding, *Biophys. Chem. 100*, 397−407.
10. Tanford, C. (1970) Protein denaturation. Part C. Theoretical models for the mechanism of denaturation, *Adv. Protein Chem. 24*, 1−95.
11. Pohl, F. M. (1976) Temperature dependence of the kinetics of folding of chymotrypsinogen A, *FEBS Lett. 65*, 293−296.
12. Scalley, M. L., and Baker, D. (1997) Protein folding kinetics exhibit an Arrhenius temperature dependence when corrected for the temperature dependence of protein stability, *Proc. Natl. Acad. Sci. U.S.A. 94*, 10636−10640.
13. Kuhlman, B., Luisi, D. L., Evans, P. A., and Raleigh, D. P. (1998) Global analysis of the effects of temperature and denaturant on the folding and unfolding kinetics of the N-terminal domain of the protein L9, *J. Mol. Biol. 284*, 1661−1670.
14. Pappenberger, G., Saudan, C., Becker, M., Merbach, A. E., and Kiefhaber, T. (2000) Denaturant-induced movement of the transition state of protein folding revealed by high-pressure stopped-flow measurements, *Proc. Natl. Acad. Sci. U.S.A. 97*, 17−22.
15. Tan, Y. J., Oliveberg, M., and Fersht, A. R. (1996) Titration properties and thermodynamics of the transition state for folding: Comparison of two-state and multi-state folding pathways, *J. Mol. Biol. 264*, 377−389.
16. Oliveberg, M., and Fersht, A. R. (1996) Formation of electrostatic interactions on the protein-folding pathway, *Biochemistry 35*, 2726−2737.
17. Raleigh, D. P., and Plaxco, K. W. (2005) The protein folding transition state: what are φ values really telling us, *Protein Pept. Lett. 12*, 117−122.
18. Cho, J. H., and Raleigh, D. P. (2006) Denatured state effects and the origin of nonclassical φ values in protein folding, *J. Am. Chem. Soc. 128*, 16492−16493.
19. Luisi, D. L., and Raleigh, D. P. (2000) pH-dependent interactions and the stability and folding kinetics of the N-terminal domain of L9. Electrostatic interactions are only weakly formed in the transition state for folding, *J. Mol. Biol. 299*, 1091−1100.
20. Cavagnero, S., Debe, D. A., Zhou, Z. H., Adams, M. W., and Chan, S. I. (1998) Kinetic role of electrostatic interactions in the unfolding of hyperthermophilic and mesophilic rubredoxins, *Biochemistry 37*, 3369−3376.
21. Hendsch, Z. S., and Tidor, B. (1994) Do salt bridges stabilize proteins? A continuum electrostatic analysis, *Protein Sci. 3*, 211−226.
22. Lopez-Arenas, L., Solis-Mendiola, S., and Hernandez-Arana, A. (1999) Estimating the degree of expansion in the transition state for protein unfolding: Analysis of the pH dependence of the rate constant for caricain denaturation, *Biochemistry 38*, 15936−15943.
23. Tissot, A. C., Vuilleumier, S., and Fersht, A. R. (1996) Importance of two buried salt bridges in the stability and folding pathway of barnase, *Biochemistry 35*, 6786−6794.
24. Yang, A. S., and Honig, B. (1993) On the pH dependence of protein stability, *J. Mol. Biol. 231*, 459−474.
25. Spencer, D. S., Xu, K., Logan, T. M., and Zhou, H. X. (2005) Effects of pH, salt, and macromolecular crowding on the stability of FK506-binding protein: An integrated experimental and theoretical study, *J. Mol. Biol. 351*, 219−232.
26. Goto, Y., Calciano, L. J., and Fink, A. L. (1990) Acid-induced folding of proteins, *Proc. Natl. Acad. Sci. U.S.A. 87*, 573−577.
27. Kuhlman, B., Luisi, D. L., Young, P., and Raleigh, D. P. (1999) pK_a values and the pH dependent stability of the N-terminal domain of L9 as probes of electrostatic interactions in the denatured state. Differentiation between local and nonlocal interactions, *Biochemistry 38*, 4896−4903.
28. Meeker, A. K., Garcia-Moreno, B., and Shortle, D. (1996) Contributions of the ionizable amino acids to the stability of staphylococcal nuclease, *Biochemistry 35*, 6443−6449.
29. Oliveberg, M., Arcus, V. L., and Fersht, A. R. (1995) pK_a values of carboxyl groups in the native and denatured states of barnase: the pK_a values of the denatured state are on average 0.4 units lower than those of model compounds, *Biochemistry 34*, 9424−9433.
30. Pace, C. N., Alston, R. W., and Shaw, K. L. (2000) Charge−charge interactions influence the denatured state ensemble and contribute to protein stability, *Protein Sci. 9*, 1395−1398.
31. Cho, J. H., Sato, S., and Raleigh, D. P. (2004) Thermodynamics and kinetics of non-native interactions in protein folding: A single point mutant significantly stabilizes the N-terminal domain of L9 by modulating non-native interactions in the denatured state, *J. Mol. Biol. 338*, 827−837.
32. Cho, J. H., and Raleigh, D. P. (2005) Mutational analysis demonstrates that specific electrostatic interactions can play a key role in the denatured state ensemble of proteins, *J. Mol. Biol. 353*, 174−185.
33. de Los Rios, M. A., and Plaxco, K. W. (2005) Apparent Debye−Huckel electrostatic effects in the folding of a simple, single domain protein, *Biochemistry 44*, 1243−1250.
34. Otzen, D. E., and Oliveberg, M. (1999) Salt-induced detour through compact regions of the protein folding landscape, *Proc. Natl. Acad. Sci. U.S.A. 96*, 11746−11751.
35. Chen, Y. R., and Clark, A. C. (2003) Equilibrium and kinetic folding of an α-helical Greek key protein domain: caspase recruitment domain (CARD) of RICK, *Biochemistry 42*, 6310−6320.
36. Broering, J. M., and Bommarius, A. S. (2005) Evaluation of Hofmeister effects on the kinetic stability of proteins, *J. Phys. Chem. B 109*, 20612−20619.
37. Dominy, B. N., Perl, D., Schmid, F. X., and Brooks, C. L., III. (2002) The effects of ionic strength on protein stability: The cold shock protein family, *J. Mol. Biol. 319*, 541−554.

38. Scholtz, J. M., York, E. J., Stewart, J. M., and Baldwin, R. L. (1991) A neutral, water-soluble, α-helical peptide: the effect of ionic strength on the helix-oil equilibrium, *J. Am. Chem. Soc. 113*, 5102−5104.
39. Baldwin, R. L. (1996) How Hofmeister ion interactions affect protein stability, *Biophys. J. 71*, 2056−2063.
40. Zhou, H. X., and Dong, F. (2003) Electrostatic contributions to the stability of a thermophilic cold shock protein, *Biophys. J. 84*, 2216−2222.
41. Kao, Y. H., Fitch, C. A., Bhattacharya, S., Sarkisian, C. J., Lecomte, J. T., and Garcia-Moreno, E. B. (2000) Salt effects on ionization equilibria of histidines in myoglobin, *Biophys. J. 79*, 1637−1654.
42. Lee, K. K., Fitch, C. A., and Garcia-Moreno, E. B. (2002) Distance dependence and salt sensitivity of pairwise, coulombic interactions in a protein, *Protein Sci. 11*, 1004−1016.
43. Luisi, D. L., Snow, C. D., Lin, J. J., Hendsch, Z. S., Tidor, B., and Raleigh, D. P. (2003) Surface salt bridges, double-mutant cycles, and protein stability: An experimental and computational analysis of the interaction of the Asp 23 side chain with the N-terminus of the N-terminal domain of the ribosomal protein L9, *Biochemistry 42*, 7050−7060.
44. Kuhlman, B., and Raleigh, D. P. (1998) Global analysis of the thermal and chemical denaturation of the N-terminal domain of the ribosomal protein L9 in H_2O and D_2O. Determination of the thermodynamic parameters, ΔH^0, ΔS^0, and ΔC_p^0 and evaluation of solvent isotope effects, *Protein Sci. 7*, 2405−2412.
45. Kuhlman, B., Boice, J. A., Fairman, R., and Raleigh, D. P. (1998) Structure and stability of the N-terminal domain of the ribosomal protein L9: Evidence for rapid two-state folding, *Biochemistry 37*, 1025−1032.
46. Pace, C. N. S. B. A., and Thomson, J. A. (1989) Measuring the conformational stability of a protein, In *Protein Structure: A Practical Approach* (Creighton, T. E., Ed.), IRL Press, Oxford, U.K.
47. Myers, J. K., Pace, C. N., and Scholtz, J. M. (1995) Denaturant *m* values and heat capacity changes: Relation to changes in accessible surface areas of protein unfolding, *Protein Sci. 4*, 2138−2148.
48. Leffler, J. E. (1953) Parameters for the description of transition states, *Science 117*, 340−341.
49. Jencks, W. P. (1985) A primer for the Bema Hapothle. An empirical approach to the characterization of changing transition-state structure, *Chem. Rev. 85*, 511−527.
50. Anil, B., Sato, S., Cho, J. H., and Raleigh, D. P. (2005) Fine structure analysis of a protein folding transition state; distinguishing between hydrophobic stabilization and specific packing, *J. Mol. Biol. 354*, 693−705.
51. Sato, S., and Raleigh, D. P. (2007) Kinetic isotope effects reveal the presence of significant secondary structure in the transition state for the folding of the N-terminal domain of L9, *J. Mol. Biol. 370*, 349−355.

BI701645G